

Nonmagnetic-Defect-Induced Magnetism in Graphene

Hideki KUMAZAKI and Dai S. HIRASHIMA

Department of Physics, Nagoya University, Nagoya 464-8602.

(Received July 12, 2018)

It is shown that a strong impurity potential induces short-range antiferromagnetic (ferrimagnetic) order around itself in a Hubbard model on a half-filled honeycomb lattice. This implies that short-range magnetic order is induced in monolayer graphene by a nonmagnetic defect such as a vacancy with full hydrogen termination or a chemisorption defect.

KEYWORDS: graphene, vacancies, magnetic moment

Physical properties of graphene (a monolayer graphite sheet) have attracted much interest since it was fabricated,¹ magneto-transport properties were studied,^{2,3} and various peculiar properties such as the half-integer quantum Hall effect^{4–6} were found. Although the main interest is in its transport properties at present, magnetic properties are also worth studying. Indeed, interest in magnetism in carbon-based materials has recently surged because of not only its fundamental importance, but also possibility of application in new technologies.⁷

Electrons in graphene can be described by a tight-binding model on a honeycomb lattice. The purpose of this paper is to show that short-range antiferromagnetic (AF) (more precisely, ferrimagnetic) order is induced around an impurity introduced on a half-filled honeycomb lattice.

Magnetism in graphite systems has been studied in many experiments,^{8,9} although the issue has been controversial; the effect of magnetic impurities cannot be completely discarded. Apart from magnetic impurities, the defect-induced mechanism is the most probable mechanism of magnetism in carbon-based materials. For example, a free dangling bond associated with a vacancy will have a net magnetic moment, which may induce a magnetic state. Even if a defect itself is nonmagnetic, it can cause spin polarization of π electrons around it. It has been known that localized edge states are generated at a zigzag edge and they can lead to a magnetic state.^{10–12} In previous studies,^{13,14} we showed that a strong impurity potential in a half-filled honeycomb lattice induces a localized state (zero mode) around it^{15–17} and that it causes enhancement of staggered susceptibility. We did not find any (short-range) order, however, because we did not consider electron-electron interaction. In this study, considering electron-electron interaction, we show that short-range magnetic order is indeed induced around a strong-impurity site in a half-filled honeycomb lattice.

We start from a tight-binding model on a honeycomb lattice. We consider only the nearest neighbor transfer t , and then the hamiltonian is given by

$$\mathcal{H}_0 = -t \sum_{(\mathbf{n}A, \mathbf{n}'B), \sigma} [c_{\mathbf{n}A\sigma}^\dagger c_{\mathbf{n}'B\sigma} + \text{h.c.}], \quad (1)$$

where $c_{\mathbf{n}\alpha\sigma}$ ($c_{\mathbf{n}\alpha\sigma}^\dagger$) is an annihilation (creation) operator of an electron with the spin σ on sublattice α in the \mathbf{n} th unit cell, and $(\mathbf{n}A, \mathbf{n}'B)$ stands for the pairs of

the nearest sites. We denote the number of the unit cell by $N_u = L^2$. The number of the lattice points is $N_L = 2N_u = 2L^2$. In addition to \mathcal{H}_0 , we consider electron-electron interaction. We consider the on-site Coulomb interaction U . Long-range Coulomb interaction is poorly screened in graphene. However, because it must be the short-range part of the Coulomb interaction that plays the most important role in inducing magnetism, we consider only the on-site Coulomb interaction and use the following interaction hamiltonian \mathcal{H}' ,

$$\mathcal{H}' = U \sum_{\mathbf{n}, \alpha} \hat{n}_{\mathbf{n}\alpha\uparrow} \hat{n}_{\mathbf{n}\alpha\downarrow}, \quad (2)$$

where $\hat{n}_{\mathbf{n}\alpha\sigma} = c_{\mathbf{n}\alpha\sigma}^\dagger c_{\mathbf{n}\alpha\sigma}$. We thus consider a Hubbard model on the honeycomb lattice.

Furthermore, we introduce impurities. We consider a short-range impurity potential. If an impurity is on sublattice α in the \mathbf{n} th unit cell, its effect is expressed by

$$\mathcal{V}(\mathbf{n}, \alpha) = u \sum_{\sigma} c_{\mathbf{n}\alpha\sigma}^\dagger c_{\mathbf{n}\alpha\sigma}. \quad (3)$$

The limit of $u \rightarrow \infty$ represents a strong impurity such as a vacancy or a hydrogen chemisorption defect.¹⁸ In that case, the total number of the lattice points is $N_L = 2N - N_i$, where N_i is the number of impurities. We consider the half-filled case, *i.e.*, the case where the number N_e of electrons is equal to N_L , in this study. Actually, we consider the case with $N_i = 2$.

We resort to a mean field approximation. The interaction term is approximated as

$$\mathcal{H}' \simeq -U \sum_{\mathbf{n}, \alpha} \langle \hat{n}_{\mathbf{n}\alpha\uparrow} \rangle \langle \hat{n}_{\mathbf{n}\alpha\downarrow} \rangle + U \sum_{\mathbf{n}, \alpha, \sigma} \langle \hat{n}_{\mathbf{n}\alpha-\sigma} \rangle \hat{n}_{\mathbf{n}\alpha\sigma}. \quad (4)$$

The mean field hamiltonian \mathcal{H}_{mf} is then given by, apart from a c-number term,

$$\mathcal{H}_{\text{mf}} = \sum_{\mathbf{n}\alpha\sigma} \epsilon_{\mathbf{n}\alpha\sigma} \hat{n}_{\mathbf{n}\alpha\sigma} + \mathcal{H}_0 + \mathcal{V}, \quad (5)$$

where $\epsilon_{\mathbf{n}\alpha\sigma} = U \langle \hat{n}_{\mathbf{n}\alpha-\sigma} \rangle$. By diagonalizing \mathcal{H}_{mf} , we self-consistently determine $2N_L$ parameters, $\epsilon_{\mathbf{n}\alpha\sigma}$, or, equivalently, $\langle \hat{n}_{\mathbf{n}\alpha\sigma} \rangle$, from which we can readily calculate the electron density $n_{\mathbf{n}\alpha} = \langle \hat{n}_{\mathbf{n}\alpha\uparrow} + \hat{n}_{\mathbf{n}\alpha\downarrow} \rangle$ and the spin density $m_{\mathbf{n}\alpha} = \langle \hat{n}_{\mathbf{n}\alpha\uparrow} - \hat{n}_{\mathbf{n}\alpha\downarrow} \rangle$ at each lattice point.

Before showing the results in the presence of impurities, we briefly study the impurity-free case. We define

static spin susceptibilities $\chi_{\pm}(\mathbf{q})$ by

$$\chi_{\pm}(\mathbf{q}) = \frac{1}{N_u} \int_0^{\beta} d\tau \langle [\hat{m}_A(\mathbf{q}, \tau) \pm \hat{m}_B(\mathbf{q}, \tau)] \times [\hat{m}_A(-\mathbf{q}, 0) \pm \hat{m}_B(-\mathbf{q}, 0)] \rangle, \quad (6)$$

where

$$\hat{m}_{\alpha}(\mathbf{q}) = \sum_{\mathbf{k}} (c_{\mathbf{k}-\mathbf{q}\alpha\uparrow}^{\dagger} c_{\mathbf{k}-\mathbf{q}\alpha\uparrow} - c_{\mathbf{k}-\mathbf{q}\alpha\downarrow}^{\dagger} c_{\mathbf{k}-\mathbf{q}\alpha\downarrow}). \quad (7)$$

$\chi_{+}(0)$ is uniform susceptibility and $\chi_{-}(0)$ is staggered susceptibility. In Fig. 1, we show the momentum dependence of $\chi_{\pm}(\mathbf{q})$ for $U = 0$ at absolute zero, $T = 0$. It can be seen that staggered susceptibility $\chi_{-}(\mathbf{q} = 0)$ takes the maximum value.

In the random phase approximation (RPA), spin susceptibilities can be written as

$$\chi_{\pm}(\mathbf{q}) = \frac{\chi_{\pm}^{(0)}(\mathbf{q})}{1 - \frac{U}{2}\chi_{\pm}^{(0)}(\mathbf{q})}, \quad (8)$$

from which we can see that the paramagnetic state is unstable towards an AF state at $U \geq U_{\text{cr}}^{(0)} = 2/\chi_{-}^{(0)}(0) \simeq 2.23t$.

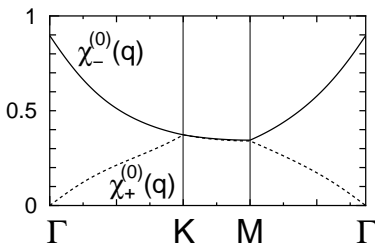


Fig. 1. Momentum dependence of spin susceptibilities $\chi_{+}(\mathbf{q})$ (dotted curve) and $\chi_{-}(\mathbf{q})$ (solid curve) of the half-filled honeycomb lattice at $U = 0$ and $T = 0$.

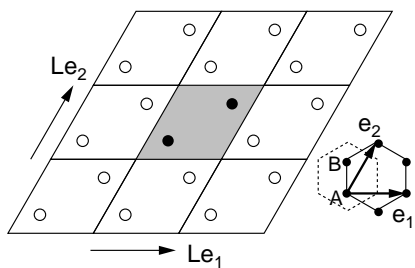


Fig. 2. Honeycomb lattice of size $L \times L$ used in calculations. The periodic boundary condition is imposed. Solid dots represent the positions of the unit cells where impurities are placed, and open dots are their images. \mathbf{e}_i ($i = 1, 2$) is the unit vector of length a , where a is the lattice constant. The dotted line shows a unit cell which includes an A sublattice point and a B sublattice point.

Now, we study the impurity effect using a finite size lattice. The lattice with $L \times L$ unit cells is shown in Fig. 2. We place two impurities in the unit cells at $\mathbf{n}_1 =$

(n_1, n_1) and $\mathbf{n}_2 = \mathbf{n}_1 + (L/2, L/2)$, and impose the periodic boundary condition. As can be seen from Fig. 2, the (shortest) distance between the two impurity sites is $L/2$.

First, we study the case with $u \rightarrow \infty$, *i.e.*, $N_L = 2N_u - 2$, and deal with the case where both impurities are on the same sublattice, say sublattice A; we denote this case by (A,A). In this case, the ground state is four-fold degenerate at $U = 0$, because four degenerate zero modes $\phi_{0\sigma}^{(k)}(\mathbf{r})$ ($\sigma = \uparrow, \downarrow$ and $k = 1, 2$) appear just at the chemical potential μ (see Fig. 3 (a)). At a finite U , two of the zero modes are occupied by equal spins in the ground state (Hund's rule), that is, the ground state always has a total moment $M_t = m_A + m_B = 2$ where m_{α} is the total moment of the sublattice α , $m_{\alpha} = \sum_{\mathbf{n}} (n_{\mathbf{n}\alpha\uparrow} - n_{\mathbf{n}\alpha\downarrow})$. This conclusion is in harmony with Lieb's theorem.¹⁹ Because the zero-mode wave function $\phi_{0\sigma}^{(k)}(\mathbf{r})$ is localized around impurity sites, the spin density is also localized around impurity sites. In Fig. 4, we show the spin density around an impurity site. It can be seen that short-range ferrimagnetic order is induced around the impurity site and that the spin density on sublattice B is larger than that on sublattice A, the sublattice where the impurity is.²⁰ As a finite total moment M_t implies, the direction of the net spin density around one impurity site is parallel with that around the other impurity site. This is easily understood as a manifestation of the dominant AF tendency of the impurity-free half-filled honeycomb lattice. The net majority moments around both impurities are mainly on sublattice B, and the nearest-neighbor AF interaction implies a ferromagnetic interaction between spins on the same sublattice. We show the dependence of the moment at each lattice point on the distance from impurity sites in Fig. 5 (a). It can indeed be seen that the moment is localized around impurities and ferrimagnetic short-range order develops.

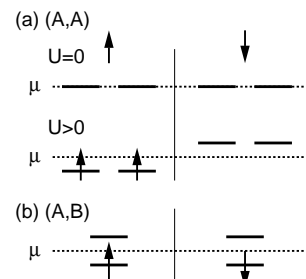


Fig. 3. The ground state spin configuration in the presence of two vacancies (a) on one of the sublattices and (b) on sublattices A and B. (a) At $U = 0$, four zero modes (two per each spin) appear at the chemical potential μ . At $U > 0$, two of them are occupied by equal spins (up spins in this figure). (b) Zero modes appear symmetrically around the chemical potential μ , and two of them are occupied by an up-spin and a down-spin.

The dependence of the square of staggered moment $M_s = m_A - m_B$ on U is shown in Fig. 6; M_s smoothly changes from 2 as U increases from zero. Total sublattice moments m_A and m_B are given by $m_A = (2 + M_s)/2$ and $m_B = (2 - M_s)/2$ ($M_s < 0$). This means that no moment

is induced on sublattice A as $U \rightarrow 0$. This is because the zero-mode wave function vanishes on sublattice A.^{14,15} The sublattice moment on sublattice A is induced by a finite U . This can be also seen in Figs. 4 (b) and 5 (a). The local moment $M_t^\ell(\ell_{\max})$, defined by $M_t^\ell(\ell_{\max}) = \sum_n (m_{nA} - m_{nB})$ where the summation is restricted to those lattice points within the distance of $\ell_{\max}a$ from an impurity site, is also shown as a function of U in Fig. 7. In contrast to the staggered moment M_s , the local moment varies only modestly.²¹ It is the staggered moment that is enhanced by the interaction.

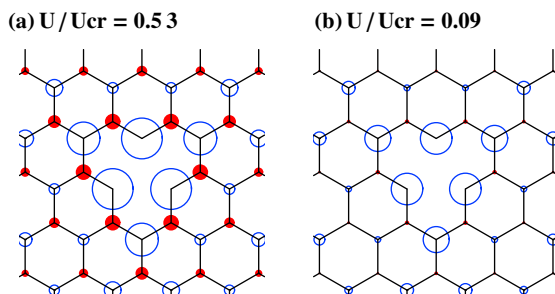


Fig. 4. Spin density around an impurity site at (a) $U = 1.2t = 0.53U_{\text{cr}}^{(0)}$ and (b) $U = 0.2t = 0.09U_{\text{cr}}^{(0)}$ for $L = 50$. Area of each dot is proportional to the magnitude of the spin density at each lattice point. Open dots represent positive magnetic moments and filled dots negative magnetic moments.

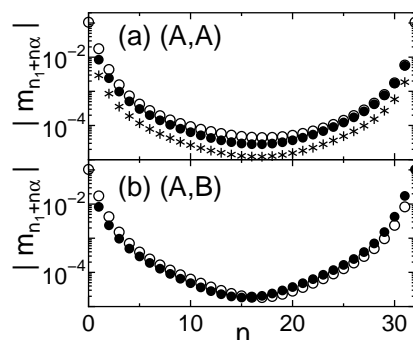


Fig. 5. Moments $-m_{n'A}$ (solid dots) and $m_{n'B}$ (open dots) in the unit cells at $n' = n_1 + (n, n)$ at $U = 1.0t$ for $L = 64$. (a) Impurities are on the A sublattice points at n_1 and at $n_1 + (32, 32)$. For comparison, $-m_{n'A}$ at $U = 0.5t$ is also shown (stars). (b) Impurities are on the A sublattice point at n_1 and on the B sublattice point at $n_1 + (32, 32)$.

Next, we study the case where one vacancy is on sublattice A, and the other is on sublattice B; we denote this case by (A,B). In this case, the zero modes appear pairwise above and below the chemical potential (see Fig. 3 (b)). At any U , two of the zero modes are occupied by up- and down-spins and the total moment M_t always vanishes in harmony with Lieb's theorem.¹⁹ At $U = 0$, the occupied zero-mode wave function $\phi_{0\sigma}^{(-)}(\mathbf{r})$ takes a finite value only on sublattice α around an impurity site on sublattice $\bar{\alpha}$.^{14,22} The spin density at each site vanishes,

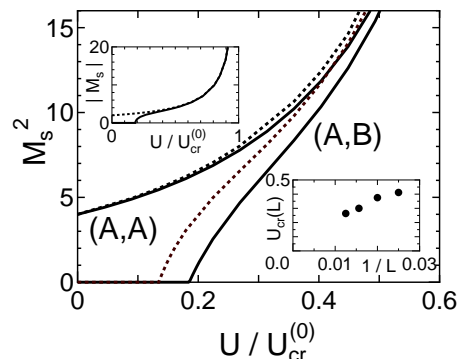


Fig. 6. The dependence of the square of staggered moment M_s on the interaction strength U ; the linear size of the lattice is $L = 40$ (solid curves) and $L = 64$ (dotted curves). M_s varies smoothly in the case (A,A) where both impurities are on sublattice A, while it evolves from zero at an L -dependent critical $U_{\text{cr}}(L)$ in the case (A,B) where one impurity is on sublattice A and the other is on sublattice B. The upper inset shows the dependence of M_s on U in a wider range for $L = 40$. The lower inset shows the dependence of $U_{\text{cr}}(L)$ on $1/L$. The critical value $U_{\text{cr}}^{(0)}$ for the bulk honeycomb lattice is $U_{\text{cr}}^{(0)} = 2.23t$.

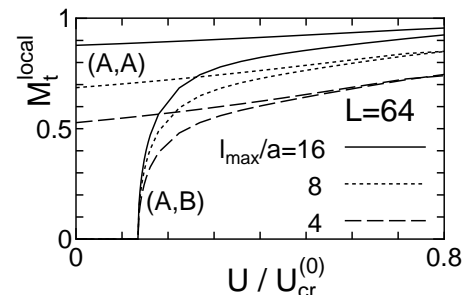


Fig. 7. Local spin moment $M_t^\ell(\ell_{\max})$ as a function of U for $L = 40$: $\ell_{\max} = 16a$ (solid curves), $8a$ (dotted curves), and $4a$ (dashed curves).

because $\phi_{0\uparrow}^{(-)}(\mathbf{r}) = \phi_{0\downarrow}^{(-)}(\mathbf{r})$. As U increases, this identity is violated. For example, $|\phi_{0\uparrow}^{(-)}(\mathbf{r})|$ takes a larger value on sublattice B than $|\phi_{0\downarrow}^{(-)}(\mathbf{r})|$, and vice versa on sublattice A. This results in a net up spin density around the impurity site on sublattice A and a net down spin density around the impurity site on sublattice B. The spin density around an impurity site at $U = 1.2t$ is very similar to the one in the case (A,A) at the same value of U , *i.e.*, Fig. 4 (a). We again find short-range ferrimagnetic order around a vacancy site. See also Fig. 5 (b). In this case, the induced net moment around the impurity site on sublattice A is antiparallel to that around the impurity site on sublattice B. This is also understood as a result of the inherent AF tendency of the half-filled honeycomb lattice. Actually, the net moment induced around one impurity is equal in magnitude with that induced around the other impurity.

We find that, for a finite L , the linear size of the lattice, there is a critical value of U , $U_{\text{cr}}(L)$, above which staggered moment takes a finite value, as can be seen from Fig. 6. Near $U_{\text{cr}}(L)$, the dependence of M_s is well

approximated as $M_s \propto \sqrt{U - U_{\text{cr}}(L)}$. The dependence of $U_{\text{cr}}(L)$ on L is shown in one of the insets of Fig. 6. The previous results^{13,14} strongly suggested that the staggered susceptibility on the non-interacting half-filled honeycomb lattice diverges in the presence of a strong impurity potential. This implies that $U_{\text{cr}}(L)$ vanishes as $L \rightarrow \infty$, that is, a finite staggered moment is induced by an infinitesimally small value of U . Moreover, as can be seen from Fig. 6, the $|M_s| - U$ curve in the (A,B) case merges that in the (A,A) case as U increases, and it merges at a smaller U at a larger L . This also implies that $U_{\text{cr}}(L)$ vanishes as $L \rightarrow \infty$. Indeed, it will make no difference whether two impurities are on the same sublattice or on the different sublattices, if the distance between them goes to infinity. From these arguments,²³ it is clear that $U_{\text{cr}}(L \rightarrow \infty)$ vanishes, although we cannot definitely confirm $U_{\text{cr}}(L \rightarrow \infty) = 0$ from the present calculation because of the limited size of the used lattice. The dependence of the local moment $M_t^\ell(\ell_{\text{max}})$ on U is shown in Fig. 7. It also merges $M_t^\ell(\ell_{\text{max}})$ in the (A,A) case as U increases.

The local moment formation is closely related to the presence of the zero modes, *i.e.*, it is specific to the half-filled honeycomb lattice. By doing similar calculations for an off-half-filled honeycomb lattice and a half-filled square lattice (without nesting), we indeed find that no local moment formation occurs at U much smaller than $U_{\text{cr}}^{(0)}$. Vacancies on the same sublattice points in a row generate a zigzag edge (and a bearded edge) where ferrimagnetic order is realized.^{10,12} This order at a zigzag edge is thus closely connected to the short-range order around a vacancy studied here.

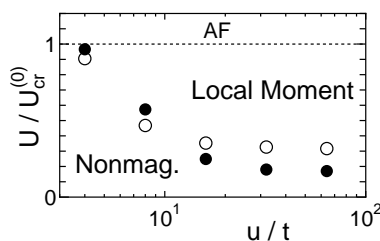


Fig. 8. Region where local moments are formed on the $u - U$ plane in the (A,B) case obtained for $L = 20$ (open dots) and 50 (filled dots). Electron number N_e is equal to $N_L - N_i = N_L - 2$. At $U > U_{\text{cr}}^{(0)}$, the AF state is realized.

Finally, we briefly discuss the case with finite u . In Fig. 8, we show the region where a local moment is formed around an impurity site in the case (A,B). At $u \gtrsim 10$, results converge to those at $u \rightarrow \infty$. At smaller u , the region where a local moment is formed is rather limited. Finite size effects are clearly seen, and the detailed study of them is left for a future study.

Now, we discuss the applicability of the present result to actual graphene. We do not know the precise value of U appropriate for graphene, and it is also difficult to estimate the value of u that represents the effect of a defect. Moreover, we have neglected the effect of long-range part of the Coulomb interaction and the possible local

distortion around a defect. Yazyev and Helm recently found ferrimagnetic short-range order around a vacancy and also around a hydrogen chemisorption defect using a first-principles calculation.²⁴ This implies that actual graphene with nonmagnetic defects is in the region of Fig. 8 where local moments develop around impurities and that the short-range order is caused by the same mechanism discussed in this work.

We find that the energy gain per vacancy due to the moment formation is approximately $0.01t$,²⁵ *i.e.*, 300 K in graphene. This implies that it is difficult to observe local moment formation around a single vacancy at room temperatures, and that it can be observed only at low temperatures. It is possible that a moment develops more stably near a few defects close to each other. This is also a subject of a future study.

A local magnetic moment can also be formed around a defect in other carbon-based materials. For example, oscillation of spin density was found around a vacancy in a (10,0) carbon nanotube with a first-principles calculation.²⁶ This may also be caused by the same mechanism discussed here.

To conclude, we have studied the effect of nonmagnetic defects on magnetism of electrons on the half-filled honeycomb lattice and found that short-range ferrimagnetic order is induced and a local moment is formed around a defect. This strongly implies that a nonmagnetic defect in graphene indeed induces a local magnetic moment around it.

We would like to thank Dr. K. Wakabayashi and Dr. O. V. Yazyev for useful discussions and correspondence. This work was supported in part by Research Foundation for the Electrotechnology of Chubu.

- 1) K. S. Novoselov, A. K. Geim, S. V. Morozov, D. Jiang, Y. Zhang, S. V. Dubonos, I. V. Grigorieva and A. A. Firsov: *Science* **306** (2004) 666.
- 2) K. S. Novoselov, A. K. Geim, S. V. Morozov, D. Jiang, M. I. Katsnelson, I. V. Grigorieva, S. V. Dubonos and A. A. Firsov: *Nature* **438** (2005) 197.
- 3) Y. Zhang, Y.-W. Tan, H. L. Stormer and P. Kim: *Nature* **438** (2005) 201.
- 4) Y. Zheng and T. Ando: *Phys. Rev. B* **65** (2002) 245420.
- 5) V. P. Gusynin and S. G. Sharapov: *Phys. Rev. Lett.* **95** (2005) 146801.
- 6) N. M. R. Peres, F. Guinea and A. H. Castro Neto: *Phys. Rev. B* **73** (2006) 125411.
- 7) *Carbon-based Magnetism: An Overview of the Magnetism of Metal Free Carbon-based Compounds and Materials*, edited by T. L. Marakova and F. Palacio, Elsevier Science, North Holland, 2006.
- 8) Y. Shibayama, H. Sato, T. Enoki and M. Endo: *Phys. Rev. Lett.* **84** (2000) 1744.
- 9) P. Esquinazi, A. Setzler, R. Höne, C. Semmelhack, Y. Kopelevich, D. Spemann, T. Butz, B. Kohlstrunk and M. Lösche: *Phys. Rev. B* **66** (2002) 024429, and references therein.
- 10) M. Fujita, K. Wakabayashi, K. Nakada and K. Kusakabe: *J. Phys. Soc. Jpn.* **65** (1996) 1920.
- 11) K. Nakada, M. Fujita, G. Dresselhaus and M. S. Dresselhaus: *Phys. Rev. B* **54** (1996) 17954.
- 12) S. Okada and A. Oshiyama: *J. Phys. Soc. Jpn.* **72** (2003) 1510.
- 13) H. Kumazaki and D. S. Hirashima: *J. Phys. Soc. Jpn.* **75** (2006) 053707.
- 14) H. Kumazaki and D. S. Hirashima: *J. Phys. Soc. Jpn.* **76** (2007) 034707..

15) K. Wakabayashi: J. Phys. Soc. Jpn. **71** (2002) 2500.

16) V. M. Pereira, F. Guinea, J. M. B. Lopes dos Santos, N. M. R. Peres and A. H. Castro Neto: Phys. Rev. Lett. **96** (2006) 036801.

17) T. O. Wehling, A. V. Balatsky, M. I. Katsnelson, A. I. Lichtenstein, K. Schanberg and R. Wiesendanger: cond-mat/0609503.

18) A chemisorbed hydrogen atom is mobile, but we do not consider the mobility here.

19) E. H. Lieb: Phys. Rev. Lett. **62** (1989) 1201.

20) Charge density is found to be uniform except for the impurity sites, although the spin density spatially varies.

21) If we sum the moments in the half of the total lattice points, *i.e.*, in the rectangle with side-lengths $L/2$ and $\sqrt{3}L/2$ around an impurity, the local moment is unity for any U .

22) The zero-mode wave function on sublattice α around an impurity site on sublattice α does not vanish exactly, but is negligibly small and tends to vanish when the distance between the two impurities goes to infinity.

23) At $L \rightarrow \infty$, the four zero modes becomes degenerate at $U = 0$ as in the (A,A) case, and the local moments will be induced by an infinitesimally small U .

24) O. V. Yazyev and L. Helm: cond-mat/0610638.

25) The energy gain per vacancy is $0.0104t$ at $U = 1.0t$ for $L = 64$ in the (A,B) case.

26) Y. Ma, P. O. Lehtinen, A. S. Foster and R. M. Nieminen: Phys. Rev. B **72** (2005) 085451.